7

Axial field configurations

In this chapter, we consider field configurations that have an axial field component. In straight channels, these fields are azimuthally symmetric around the system axis and only have axial and radial components. The basic example of this type of configuration is the closed circular current loop. Combinations of current loops can be used to produce desired axial field profiles. The current loop can also be extended axially to generate an ideal sheet solenoid. We conclude the chapter with a discussion of bent solenoids. When the bent channel forms a closed ring, we obtain the toroid configuration.

7.1 Circular current loop

We recall from Equation 1.18 that the on-axis field of a circular current loop with radius a is

$$B_z = \frac{\mu_0 I a^2}{2\{a^2 + z_o^2\}^{3/2}}, \tag{7.1}$$

where I is the current in the loop and z_o is the distance of the observation point along the z axis from the plane of the loop. We now consider the determination of the vector potential in the case when the observation point P is not restricted to lie along the z axis, as shown in Figure 7.1. We define a coordinate system where the x axis lies directly below the observation point P. By symmetry, the vector potential only has a ϕ component and cannot depend on the azimuthal coordinate ϕ. The vector potential is given by

$$A_\phi(\rho, z) = \frac{\mu_0 I}{4\pi} \oint \frac{ds}{R}.$$

https://doi.org/10.1017/9781009291156.008 Published online by Cambridge University Press

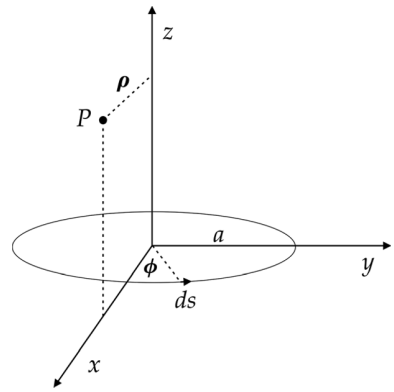

Figure 7.1 Current loop geometry.

An arbitrary element of current has the Cartesian coordinates $(a\cos\phi, a\sin\phi, 0)$, so

$$R = \left\{(\rho - a\cos\phi)^2 + (a\sin\phi)^2 + z^2\right\}^{1/2}$$
$$= \left\{\rho^2 + a^2 - 2a\rho\cos\phi + z^2\right\}^{1/2}.$$

The contribution from a current element at ϕ makes the same contribution to the vector potential as the element at $-\phi$. In addition, the contribution of each of these elements to the vector potential at P is proportional to $\cos\phi$. Therefore we can write

$$A_\phi(\rho, z) = \frac{\mu_0 I}{2\pi}\int_0^\pi \frac{\cos\phi}{\left\{\rho^2 + a^2 - 2a\rho\cos\phi + z^2\right\}^{1/2}} a\, d\phi.$$

Making the substitutions

$$\phi = \pi + 2\theta$$
$$\cos\phi = -1 + 2\sin^2\theta,$$

we can write the vector potential as

$$A_\phi(\rho, z) = \frac{\mu_0 I a}{2\pi}\int_{-\pi/2}^0 \frac{2\sin^2\theta - 1}{\left\{\rho^2 + a^2 + z^2 - 2a\rho(2\sin^2\theta - 1)\right\}^{1/2}} 2\, d\theta.$$

The integral is symmetric in θ, so we can translate the limits of integration. After rearranging the terms in the denominator, we get

$$A_\phi(\rho, z) = \frac{\mu_0 I a}{\pi}\int_0^{\pi/2} \frac{2\sin^2\theta - 1}{\left\{(a+\rho)^2 + z^2 - 4a\rho\sin^2\theta\right\}^{1/2}}\, d\theta.$$

https://doi.org/10.1017/9781009291156.008 Published online by Cambridge University Press

Define

$$k^2 = \frac{4a\rho}{(a+\rho)^2 + z^2}. \tag{7.2}$$

Then we have

$$\begin{aligned} A_\phi(\rho, z) &= \frac{\mu_0 I a}{\pi} \frac{k}{\sqrt{4a\rho}} \int_0^{\pi/2} \frac{2\sin^2\theta - 1}{\{1 - k^2\sin^2\theta\}^{1/2}} d\theta \\ &= \frac{\mu_0 I a}{\pi} \frac{k}{\sqrt{4a\rho}} [2\,\mathbb{I}_1 - \mathbb{I}_2], \end{aligned} \tag{7.3}$$

where[1]

$$\begin{aligned} \mathbb{I}_1 &= \int_0^{\pi/2} \frac{\sin^2\theta}{\{1 - k^2\sin^2\theta\}^{1/2}} \, d\theta \\ &= \frac{K(k) - E(k)}{k^2} \end{aligned}$$

and[2]

$$\begin{aligned} \mathbb{I}_2 &= \int_0^{\pi/2} \frac{1}{\{1 - k^2\sin^2\theta\}^{1/2}} \, d\theta \\ &= K(k). \end{aligned}$$

The function $K(k)$ is the complete elliptic integral of the first kind and $E(k)$ is the complete elliptic integral of the second kind.[3] Substituting back into Equation 7.3, we find

$$A_\phi(\rho, z) = \frac{\mu_0 I a}{\pi} \frac{k}{\sqrt{4a\rho}} \left[\left(\frac{2}{k^2} - 1 \right) K(k) - \frac{2}{k^2} E(k) \right],$$

which can be written in the form [1, 2]

$$A_\phi(\rho, z) = \frac{\mu_0 I}{\pi k} \sqrt{\frac{a}{\rho}} \left[\left(1 - \frac{k^2}{2} \right) K(k) - E(k) \right]. \tag{7.4}$$

[1] GR 8.112.5. [2] GR 8.112.1. [3] Properties of complete elliptic integrals are discussed in Appendix F.

https://doi.org/10.1017/9781009291156.008 Published online by Cambridge University Press

The components of the magnetic field in cylindrical coordinates are

$$B_\rho = -\frac{\partial A_\phi}{\partial z}$$
$$B_\phi = 0$$
$$B_z = \frac{1}{\rho}\,\frac{\partial}{\partial \rho}(\rho A_\phi).$$

In order to evaluate these field components, we need the derivatives of the parameter k defined in Equation 7.2. We have [1]

$$\begin{aligned}\frac{\partial k}{\partial z} &= -\frac{zk^3}{4a\rho}\\ \frac{\partial k}{\partial \rho} &= \frac{k}{2\rho} - \frac{k^3}{4\rho} - \frac{k^3}{4a}.\end{aligned} \tag{7.5}$$

We also need the derivatives[4] of the complete elliptic integrals $K(k)$ and $E(k)$ with respect to their parameter k.

$$\begin{aligned}\frac{\partial K}{\partial k} &= \frac{E}{k\ (1-k^2)} - \frac{K}{k}\\ \frac{\partial E}{\partial k} &= \frac{E}{k} - \frac{K}{k}.\end{aligned} \tag{7.6}$$

Evaluating the derivatives together with a lot of algebra,[5] we find that [1, 2]

$$B_\rho = \frac{\mu_0 I}{2\pi}\,\frac{z}{\rho\{(a+\rho)^2+z^2\}^{1/2}}\left[-K(k) + \frac{a^2+\rho^2+z^2}{(a-\rho)^2+z^2}\,E(k)\right] \tag{7.7}$$

and

$$B_z = \frac{\mu_0 I}{2\pi}\,\frac{1}{\{(a+\rho)^2+z^2\}^{1/2}}\left[K(k) + \frac{a^2-\rho^2-z^2}{(a-\rho)^2+z^2}\,E(k)\right]. \tag{7.8}$$

In the limit $\rho \to 0$, $k^2 = 0$ and the elliptic integrals in Equation 7.8 equal $\pi/2$. Then it is straightforward to show that B_z approaches Equation 7.1 for the axial field on the axis. Using l'Hopital's rule and the series expansions

[4] GR 8.123.2,4. [5] A computer algebra program is really useful here!

https://doi.org/10.1017/9781009291156.008 Published online by Cambridge University Press

$$E(k) \simeq \frac{\pi}{2} - \frac{\pi}{8}\, k^2 + \cdots$$

$$K(k) \simeq \frac{\pi}{2} + \frac{\pi}{8}\, k^2 + \cdots,$$

it is also possible to show that Equation 7.7 for B_ρ approaches 0 on the axis, as it should.

In the preceding derivation, we have gone through a standard approach of calculating the vector potential and taking its derivatives to find the field components. We have done this to illustrate several useful mathematical properties involving the use of elliptic integrals. We should note, however, that it is possible in this case to solve the Biot-Savart equation for the fields directly since the required integrals are known.[3]

Besides the solution given here in terms of $K(k)$ and $E(k)$ and cylindrical coordinates, the problem of the circular current loop has been solved using a number of alternative methods. The vector potential for the circular loop can be written in terms of Bessel functions as [4]

$$A_\phi(\rho, z) = \frac{\mu_0 I\, a}{2} \int_0^\infty J_1(ka)\, J_1(k\rho)\, e^{-k|\,z\,|}\, dk. \tag{7.9}$$

For some applications, it is more convenient to solve for the vector potential of the current loop in spherical coordinates. Spherical solutions for the vector potential and field have also been given in terms of elliptic integrals.[5, 6] However in spherical coordinates, it is sometimes more natural to expand the solutions in Legendre functions. The vector potential for the current loop for $r < a$ is given in this case as [1]

$$A_\phi(r, \theta) = \frac{\mu_0 I}{2} \sum_{n=1}^{\infty} \frac{\sin\alpha}{n(n+1)} \left(\frac{r}{a}\right)^n P_n^1(\cos\alpha)\, P_n^1(\cos\theta), \tag{7.10}$$

where P_n^1 is an associated Legendre function and α is the polar angle of the loop. For $r > a$, the radial factor in this equation must be replaced with

$$\left(\frac{a}{r}\right)^{n+1}.$$

This type of expansion makes it easier to show that the field of the current loop approaches that for a magnetic dipole in the limit when $r >> a$. It is also possible to solve for the field components directly from Maxwell's equations.[7]

https://doi.org/10.1017/9781009291156.008 Published online by Cambridge University Press

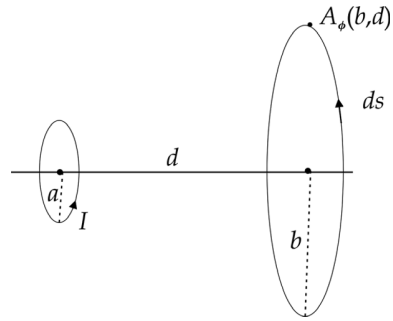

Figure 7.2 Mutual inductance of two current loops.

Example 7.1: mutual inductance of two coaxial current loops
Consider two coaxial current loops separated by a distance d, as shown in Figure 7.2. The mutual inductance between the two loops is the flux intercepted by loop 2 for a given current in loop 1. Thus we have

$$M = \frac{\Phi_2}{I_1} = \frac{1}{I_1}\int A_{\phi 1}(b,d)\, ds_2.$$

The vector potential for loop 1 at points along loop 2 can be found using Equation 7.4

$$A_\phi(b,d) = \frac{\mu_0 I}{\pi k}\sqrt{\frac{a}{b}}\left[\left(1-\frac{k^2}{2}\right)K(k) - E(k)\right],$$

where k^2 follows from Equation 7.2.

$$k^2 = \frac{4ab}{(a+b)^2 + d^2}.$$

Since the value of A_ϕ is constant for all the points on loop 2, the mutual inductance is [8]

$$M = \mu_0\sqrt{ab}\left[\left(\frac{2}{k} - k\right)K(k) - \frac{2}{k}\,E(k)\right]. \tag{7.11}$$

7.2 Radial expansion of the on-axis magnetic field

Consider a longitudinal distribution of azimuthally symmetric current sources. It is useful in some cases to express the off-axis values of the magnetic field as a function of the magnetic field along the system axis of the current distribution. This could be used, for example, to synthesize some desirable field distribution or

https://doi.org/10.1017/9781009291156.008 Published online by Cambridge University Press

for rapid optimization of current source parameters. We begin by assuming we have a scalar potential

$$\Omega = \mu_0 V_m$$

that does not depend on the coordinate ϕ and can be written as the power series

$$\Omega(\rho, z) = \sum_{n=0}^{\infty} c_n(z)\, \rho^n.$$

We demand that Ω satisfy Laplace's equation in the region from the axis up to the location of the closest coil

$$\nabla^2 \Omega = 0,$$

where the Laplacian operator is given in cylindrical coordinates by

$$\nabla^2 = \frac{1}{\rho}\, \partial_\rho(\rho\ \partial_\rho) + \partial_z^2.$$

Substituting the series for Ω into Laplace's equation and bringing the operator inside the summation sign, we get

$$\sum\nolimits_n \left[c_n\, n^2 \rho^{n-2} + \rho^n\, \frac{\partial^2 c_n}{\partial z^2} \right] = 0.$$

In order to satisfy this relation, we need to get cancellations between the c_n terms of order n and second derivative terms two orders higher than n. Therefore let us demand that

$$c_{n+2}(n+2)^2 \rho^n = -\rho^n\, \frac{\partial^2 c_n}{\partial z^2}.$$

Making the substitution $n \rightarrow n-2$, we can write the coefficient in terms of the recursion relation

$$c_n = -\frac{1}{n^2}\, \frac{\partial^2 c_{n-2}}{\partial z^2}, \qquad n \geq 2. \tag{7.12}$$

We know that the radial component of the magnetic field has to vanish on the axis of the system. Since

$$B_\rho = -\frac{\partial \Omega}{\partial \rho},$$

https://doi.org/10.1017/9781009291156.008 Published online by Cambridge University Press

we find that

$$-B_\rho = c_1 + 2c_2\,\rho + 3c_3\,\rho^2 + \cdots$$

Therefore, we must have $c_1 = 0$, and since Equation 7.12 relates c_1 to all the higher odd terms, the series expansion for Ω can only contain even terms. Thus Ω has the form

$$\Omega(\rho, z) = \sum_{n=0}^{\infty} c_{2n}(z)\,\rho^{2n},$$

where

$$c_{2n}(z) = \frac{(-1)^n \dfrac{\partial^{2n} c_0}{\partial z^{2n}}}{2^{2n}(n!)^2}. \tag{7.13}$$

The numerical factors in the coefficient can be checked by comparing the values from Equation 7.13 with the values from recursively using Equation 7.12. Define the magnetic field on the system axis as

$$B_0(z) = B_z(0, z) = -\left.\frac{\partial \Omega}{\partial z}\right|_{\rho=0} = -\frac{\partial c_0}{\partial z}.$$

Then the off-axis axial field component is [9]

$$B_z(\rho, z) = \sum_{n=0}^{\infty} \frac{(-1)^n}{2^{2n}(n!)^2} \frac{\partial^{2n} B_0}{\partial z^{2n}}\,\rho^{2n} \tag{7.14}$$

and the off-axis radial field component is

$$B_\rho(\rho, z) = \sum_{n=0}^{\infty} \frac{(-1)^{n+1}}{2^{2n+1} n!(n+1)!} \frac{\partial^{2n+1} B_0}{\partial z^{2n+1}}\,\rho^{2n+1}. \tag{7.15}$$

In cases involving loops and solenoids, where the on-axis fields are known analytically, it is possible using this method to achieve high accuracy in computing the field out to radial distances ~70% of the coil radius.[9]

7.3 Zonal harmonic expansions

The solution of Laplace's equation in spherical coordinates for azimuthally symmetric current distributions can be expressed as a series of *zonal harmonic*

https://doi.org/10.1017/9781009291156.008 Published online by Cambridge University Press

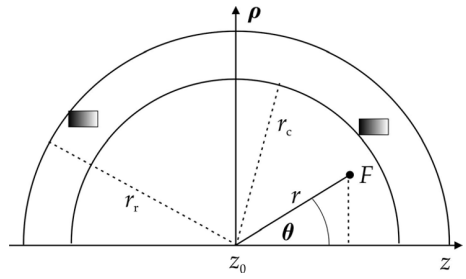

Figure 7.3 Geometry for zonal harmonic calculations.

functions.[10, 11] Computations of magnetic fields using these expansions can be faster than calculations using elliptic integrals. In addition, the harmonic expansion allows easier optimization, where, for example, we can get better field quality by eliminating leading error terms in the series.

Consider the spherical coordinate system shown in Figure 7.3. The z axis is the polar axis of symmetry. We choose a *source point* z_0 along the z axis as the origin of the coordinate system. We define a *central region* extending from the origin to a radius r_c that is the shortest distance to the edge of any current element. We define the *remote region* to extend from the radius r_r, which is the longest distance from the origin to any part of a current element, to infinity. The zonal harmonic expansion can be written as convergent series for $r < r_c$ and for $r > r_r$. The expansion for a given source point is divergent in the region $r_c < r < r_r$. However, it is possible to extend the region of validity by moving the source point. The conductors are azimuthally symmetric around the z axis. The field point F is defined to have the spherical coordinates r and θ.

The magnetic scalar potential $V = V_m$ is a solution of Laplace's equation. Let us define $u = \cos\theta$. The zonal harmonic solution in the central region is

$$V = \sum_{n=0}^{\infty} c_n \, r^n P_n(u),$$

where $P_n(u)$ is the Legendre polynomial[6] of order n. We choose to write the coefficients c_n in the following manner in order to simplify the expressions for the magnetic field.

$$c_0 = V(z_0)$$
$$c_n = -\frac{1}{\mu_0 n \, r_c^{n-1}} \, B^c_{n-1}, \qquad n > 0.$$

[6] Some important properties of Legendre functions are discussed in Appendix D.

https://doi.org/10.1017/9781009291156.008 Published online by Cambridge University Press

The unknown quantities are now contained in the coefficients B_n^c, which are called the *source terms* for the central region. These quantities will be related later to the fields produced by various current elements, such as circular loops. An important feature of the zonal harmonic method is that the source terms for a given z_o only depend on the coordinates of the current source. Thus once the source terms have been calculated, they can be used repeatedly in the series expansions for different field points.

With these definitions, V in the *central* region is written as [10]

$$V = V(z_o) - \frac{r_c}{\mu_0} \sum_{n=1}^{\infty} \frac{B_{n-1}^c}{n} \left(\frac{r}{r_c}\right)^n P_n(u).$$

In order to compute the cylindrical components of the magnetic field, we first make use of the following relations from Figure 7.3.

$$\begin{aligned} r &= \sqrt{\rho^2 + (z - z_o)^2} \\ \partial_z r &= u \\ \partial_\rho r &= \sin\theta \end{aligned}$$

and

$$\begin{aligned} u &= \frac{z - z_o}{r} \\ \partial_z u &= \frac{1 - u^2}{r} \\ \partial_\rho u &= -\frac{u}{r} \sin\theta. \end{aligned}$$

The axial component of the field is

$$B_z = r_c \sum_{n=1}^{\infty} \frac{B_{n-1}^c}{n\, r_c^n} \left[r^n\, P_n'(u) \left(\frac{1 - u^2}{r}\right) + P_n(u) n\, r^{n-1}\, u \right],$$

where P'_n is the derivative of P_n with respect to its argument u. The quantity in square brackets is

$$[\,] = r^{n-1} \{ P_n'(u)\,(1 - u^2) + nuP_n(u) \}.$$

We can use the recursion relation for Legendre polynomials[7]

$$(1 - u^2)\, P_n' = nP_{n-1} - unP_n \tag{7.16}$$

[7] GR 8.914.2.

https://doi.org/10.1017/9781009291156.008 Published online by Cambridge University Press

to write

$$[\,] = r^{n-1} n P_{n-1}(u).$$

Substituting back into the equation for B_z, we find

$$B_z = \sum_{n=1}^{\infty} B_{n-1}^c \left(\frac{r}{r_c}\right)^{n-1} P_{n-1}(u).$$

Changing the index to $m = n - 1$, the axial field in the central region can be written as

$$B_z = \sum_{m=0}^{\infty} B_m^c \left(\frac{r}{r_c}\right)^m P_m(u). \tag{7.17}$$

Following a similar procedure, the transverse field component in the central region is

$$B_\rho = r_c \sum_{n=1}^{\infty} \frac{B_{n-1}^c}{n\ r_c^n} [r^{n-1} \sin\theta\ (-uP'_n + nP_n)].$$

Using the recursion relation [12]

$$nP_n = uP'_n - P'_{n-1}$$

and shifting the series index again, we find the transverse field in the central region is

$$B_\rho = -\sin\theta \sum_{m=0}^{\infty} \frac{B_m^c}{m+1} \left(\frac{r}{r_c}\right)^m P'_m(u). \tag{7.18}$$

In the *remote* region, we write the scalar potential in the form

$$V = V_0(\pm\infty) + \frac{r_r}{\mu_0} \sum_{n=1}^{\infty} \frac{B_{n+1}^r}{n+1} \left(\frac{r_r}{r}\right)^{n+1} P_n(u).$$

The axial field is

$$B_z = -\sum_{n=1}^{\infty} \frac{B_{n+1}^r}{n+1} \left(\frac{r_r}{r}\right)^{n+2} \left[P'_n(1-u^2) - P_n u\ (n+1)\right].$$

Using the recursion relation Equation 7.16 and shifting the series index, we find the axial field component in the remote region is

$$B_z = \sum_{m=2}^{\infty} B_m^r \left(\frac{r_r}{r}\right)^{m+1} P_m(u). \tag{7.19}$$

https://doi.org/10.1017/9781009291156.008 Published online by Cambridge University Press

The transverse field component in the remote region is

$$B_\rho = -\sum_{n=1}^{\infty} \frac{B^r_{n+1}}{n+1} \left(\frac{r_r}{r}\right)^{n+2} \sin\theta \, \left[-uP'_n - (n+1)P_n\right].$$

Using the recursion relation [13]

$$(n+1)P_n = P'_{n+1} - uP'_n$$

and shifting the series index, we find that the transverse field component in the remote region is

$$B_\rho = \sin\theta \sum_{m=2}^{\infty} \frac{B^r_m}{m} \left(\frac{r_r}{r}\right)^{m+1} P'_m(u). \tag{7.20}$$

Now that we have determined the series representations of the field components in the central and remote regions, we turn to the calculation of the *source* terms. Consider a field point on the z axis in the central region with $z > z_o$. In this case, $\theta = 0$, $\rho = 0$, $u = 1$, and $r = z - z_o$. From Equation 7.17, we have

$$B_0(z) = B_z(0,z) = \sum_{n=0}^{\infty} \frac{B^c_n}{r^n_c} \, (z - z_o)^n.$$

When $n = 0$ and $z = z_o$, we see that the coefficient

$$B^c_0 = B_z(0, z_o)$$

is the axial magnetic field at the source point. The Taylor series around the point z_0 is

$$B_0(z) = \sum_{n=0}^{\infty} \frac{1}{n!} \, \frac{d^n B_0}{dz^n}\bigg|_{z_o} (z - z_o)^n. \tag{7.21}$$

Comparing the two series for B_0, we find that [11]

$$B^c_n = \frac{r^n_c}{n!} \, \frac{d^n B_0}{dz^n}(z_o). \tag{7.22}$$

Suppose that the current source is a circular loop, as shown in Figure 7.4. For a current loop, we have $r_c = r_r = r_L$. From Equation 7.1, the axial field at the field point F is

$$B_0(z) = \frac{\mu_0 I \rho^2_L}{2d^3}. \tag{7.23}$$

https://doi.org/10.1017/9781009291156.008 Published online by Cambridge University Press

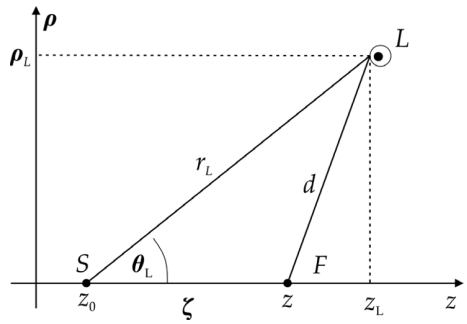

Figure 7.4 Source terms for a circular current loop.

Define $\zeta = z - z_o$. From the law of cosines, we have

$$d = \sqrt{r_L^2 + \zeta^2 - 2\ r_L\ \zeta\ u_L}.$$

We make use of the following series expansion for Legendre polynomials[8]

$$\frac{1}{\sqrt{1 + h^2 - 2hu}} = \sum_{n=0}^{\infty} h^n\ P_n(u),$$

where $h < 1$. Differentiating both sides of this equation with respect to u, we find

$$\frac{1}{\{1 + h^2 - 2hu\}^{3/2}} = \sum_{n=0}^{\infty} h^n\ P'_{n+1}(u). \tag{7.24}$$

In the central region, let

$$h = \frac{\zeta}{r_L} < 1,$$

so that

$$d = r_L \sqrt{1 + h^2 - 2\ hu_L}.$$

Using Equation 7.24, we find that

$$\frac{1}{d^3} = \frac{1}{r_L^3} \sum_{n=0}^{\infty} h^n\ P'_{n+1}(u_L).$$

[8] GR 8.921.

https://doi.org/10.1017/9781009291156.008 Published online by Cambridge University Press

Substituting this into Equation 7.23 and comparing with the general series expansion Equation 7.17 for the case of a field point on the axis, we can conclude that the source term for the circular loop in the central region is [11]

$$B_n^c = \frac{\mu_0 I \rho_L^2}{2 r_L^3} P'_{n+1}(u_L). \tag{7.25}$$

Note that this expression does not depend on any parameters of a field point. We follow an analogous procedure in the remote region to find that

$$B_n^r = \frac{\mu_0 I \rho_L^2}{2 r_L^3} P'_{n-1}(u_L). \tag{7.26}$$

7.4 Multiple coil configurations

Combinations of current loops are often used to create regions of space with some desired magnetic properties. We can generalize the current source as a "small" coil with N turns, provided the size of the coil is small compared with the separation between the coils. In this case, we replace the loop current I in the field equations with the product NI. The classic example of a multiple coil configuration is the Helmholtz pair, where two coils are used to create a region of approximately uniform field.

Consider the arrangement of two coaxial current loops shown in Figure 7.5. The two loops are perpendicular to the z axis and have the same radius a and the same current I. The axial field of each loop is given by Equation 7.1. In a coordinate system with the origin midway between the coils, the axial field of the two loops can be written

$$B_z(0,z) = \frac{\mu_0 I\, a^2}{2} F(z), \tag{7.27}$$

where

$$F(z) = \frac{1}{\{a^2 + (b-z)^2\}^{3/2}} - \frac{1}{\{a^2 + (b+z)^2\}^{3/2}}. \tag{7.28}$$

In the Helmholtz configuration, the spacing $2b$ between the coils equals the radius a of the coils. The field of a Helmholtz pair at the origin is

$$\begin{aligned} B_z(0,0) &= \frac{\mu_0 I}{a} \frac{8}{5\sqrt{5}} \\ &\simeq 0.7155 \frac{\mu_0 I}{a}. \end{aligned} \tag{7.29}$$

https://doi.org/10.1017/9781009291156.008 Published online by Cambridge University Press

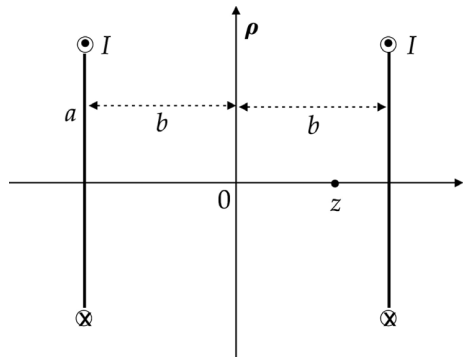

Figure 7.5 A two-coil configuration.

The axial field between the coils falls off slowly with z. At the center of the current loops the field is

$$B_z\left(0,\frac{a}{2}\right) = \frac{\mu_0 I}{a}\ \frac{1}{2}\left[1+\frac{1}{\sqrt{8}}\right]$$
$$\simeq 0.6768\ \frac{\mu_0 I}{a}\ .$$

In the vicinity of the origin, the axial field can be expanded in the Taylor series, Equation 7.21. The field uniformity is determined by the leading-order terms in this expansion. Because of the symmetry of the coil arrangement, all the odd power terms in the series have to vanish. The virtue of the Helmholtz configuration is that the second derivative term in the expansion also vanishes. Thus the leading correction in the Taylor series is the fourth order term, which is proportional to

$$\frac{\partial^4 B_z}{\partial z^4} \simeq -\ 19.8\ \frac{\mu_0 I}{a^5}.$$

Thus in the vicinity of the origin, the axial field is [14]

$$B(0,z) \simeq \frac{\mu_0 I}{a}\left[0.7155 - 0.825\left(\frac{z}{a}\right)^4 + \cdots\right]. \tag{7.30}$$

The field at any point off the axis can be found by using the elliptic integral solutions for the current loop given in Equations 7.7 and 7.8.[15] In the plane midway between the coils, the field only has an axial component because of symmetry. Defining the scaled radius $u = \rho/a$, the elliptic integral parameter is

$$k^2 = \frac{16u}{4u^2+8u+5}$$

https://doi.org/10.1017/9781009291156.008 Published online by Cambridge University Press

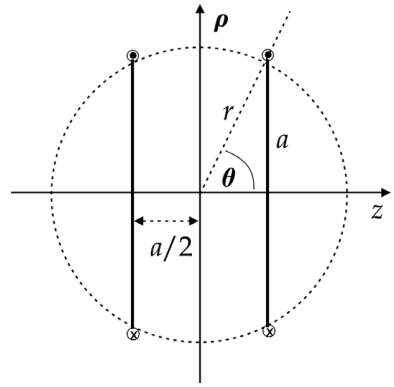

Figure 7.6 Helmholtz coil configuration.

and the axial field is

$$B_z(u,0) = \frac{2\mu_0 I}{\pi a}\,\frac{1}{\sqrt{4u^2+8u+5}}\left[K(k) + \frac{3-4u^2}{4u^2-8u+5}\,E(k)\right].$$

By numerically evaluating this expression, the field is found to be quite uniform in the vicinity of the axis.[16] It falls off to 99.93% of the on-axis value at a radius of $0.2a$.

The Helmholtz pair arrangement has the geometric property that the two coils lie on the surface of a sphere, as illustrated in Figure 7.6. For this configuration, we have

$$\tan\,\theta = 2$$
$$\sin\,\theta = \frac{a}{r},$$

so the radius of the sphere is

$$r = \frac{a}{\sin(\tan^{-1}2)} \simeq 1.118\,a.$$

The Helmholtz pair also has interesting asymptotic behavior.[17] Expanding the on-axis field in powers of a/z, the field at large distance is given by

$$B_z(0,z) \simeq \frac{\mu_0 I a^2}{z^3} + \frac{3\mu_0 I a^2}{2z^5}(4b^2 - a^2) + \cdots$$

The leading term is the magnetic dipole term. However, the next term in the series vanishes under the Helmholtz condition $a = 2b$.

An *inverse Helmholtz* pair has the currents in the two coils flowing in opposite directions. In this case, the field at the origin vanishes, and the leading multipole term is the field gradient. The optimum gradient for fixed radius a is [18]

https://doi.org/10.1017/9781009291156.008 Published online by Cambridge University Press

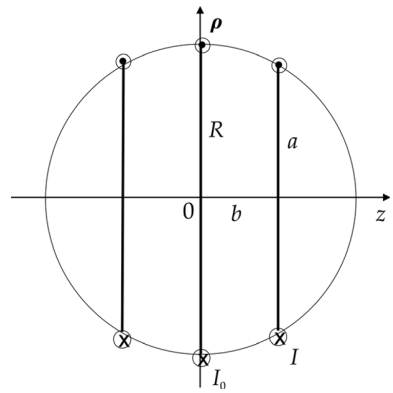

Figure 7.7 Maxwell tricoil configuration.

$$\frac{dB_z}{dz} = \frac{48}{25\sqrt{5}}\,\frac{\mu_0 I}{a^2} \simeq 0.8587\,\frac{\mu_0 I}{a^2}.$$

If practical constraints demand it, other gradient optimizations are possible for fixed spacing b or for fixed radius $r^2 = a^2 + b^2$.[19]

The classic design using three coils is the *Maxwell tricoil*, shown in Figure 7.7. The tricoil has a pair of identical coils and a third coil with larger radius in the symmetry plane between the coil pair. The three coils all lie on the surface of a sphere. This design improves on the field quality from the Helmholtz pair by also making the fourth-order term in the Taylor series vanish. Thus the first correction term is sixth-order. Maxwell's solution is

$$a = \sqrt{\frac{4}{7}}R$$

$$b = \sqrt{\frac{3}{7}}R$$

$$I = \frac{49}{64}\,I_0\,.$$

The magnetic field at the origin is

$$B_z(0,0) = 60\,\frac{\mu_0 I}{R}.$$

An improved three coil design with three circular coils of the same radius has a larger uniform field region than Maxwell's design.[15] Another sixth-order

https://doi.org/10.1017/9781009291156.008 Published online by Cambridge University Press

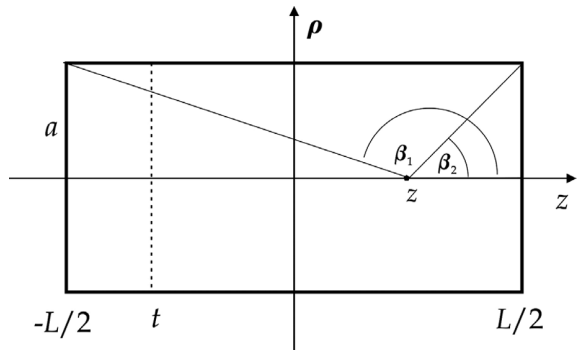

Figure 7.8 Sheet model of a solenoid.

design used three square coils.[20] An exhaustive study of multi-coil systems using the methods of zonal harmonics has identified many uniform and gradient field configurations with higher-order error corrections.[21]

7.5 Sheet model for the solenoid

We consider here the field from a solenoid in the approximation that the radial thickness of the solenoid coil can be neglected. We assume that the sheet conductor is composed of circular current loops that are extended in the axial direction for the length L of the solenoid, as shown in Figure 7.8. We compute the on-axis field at the location z of a finite length solenoid by integrating the field of a current loop

$$B_z(0,z) = \int_{-L/2}^{L/2} \frac{\mu_0 I a^2}{2\left\{a^2 + (z-t)^2\right\}^{3/2}} n\, dt\,,$$

where n is the number of turns per unit length. Performing the integration[9] gives

$$B_z(0,z) = \frac{\mu_0 nI}{2}\left[\frac{z+L/2}{\{a^2+(z+L/2)^2\}^{1/2}} - \frac{z-L/2}{\{a^2+(z-L/2)^2\}^{1/2}}\right]. \tag{7.31}$$

This can be written in the form

$$B_z(0,z) = \frac{\mu_0 nI}{2}\,(\cos\beta_2 - \cos\beta_1), \tag{7.32}$$

where β_i are the angles subtended at location z on the axis of the solenoid to the outer edges of the two ends of the current sheet. The field in the center of the solenoid is

[9] GR 2.264.5.

https://doi.org/10.1017/9781009291156.008 Published online by Cambridge University Press

$$B_z(0,0) = \mu_0 n\, I\, \frac{L}{\sqrt{L^2 + 4a^2}}. \tag{7.33}$$

In the limit of an infinitely long current sheet, this expression reduces to the field of an ideal solenoid, Equation 1.28.

$$B_z = \mu_0 n\, I.$$

There is a close connection between the derivatives of the on-axis solenoid field and the on-axis fields of the current loops at the ends of the solenoid.[9, 10] In the coordinate system in Figure 7.8,

$$\frac{dB_z^{Solenoid}(0,z)}{dz} = n\left[B_z^{Loop}\left(0, z + \frac{L}{2}\right) - B_z^{Loop}\left(0, z - \frac{L}{2}\right)\right] \tag{7.34}$$

The off-axis expansion method discussed in Section 7.2 can be used in conjunction with Equation 7.34 to find the field of a sheet solenoid.[9]

We turn next to calculating the field of a solenoid at any point, including points off the symmetry axis. We will perform a direct calculation of the field using the Biot-Savart equation

$$\overrightarrow{dB} = \frac{\mu_0 I}{4\pi}\,\frac{\overrightarrow{dl} \times \overrightarrow{R}}{R^3}.$$

Consider the solenoid geometry shown in Figure 7.9. Because of the azimuthal symmetry of the current, the field is also azimuthally symmetric. Thus for

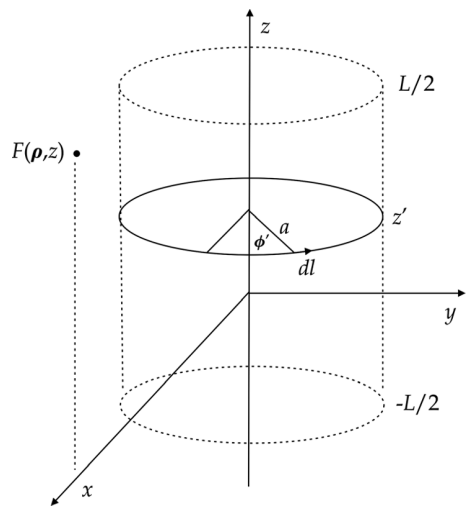

Figure 7.9 Geometry of the sheet solenoid.

https://doi.org/10.1017/9781009291156.008 Published online by Cambridge University Press

mathematical simplicity, we are free to choose the field point F to lie directly above the x axis. The distance from the source current element to the field point is

$$\overrightarrow{R} = (\rho - a\ \cos\phi')\,\hat{x} - a\ \sin\phi'\,\hat{y} + (z - z')\,\hat{z}, \tag{7.35}$$

while the current element is

$$\overrightarrow{dl} = -a\sin\phi'\,d\phi'\,\hat{x} + a\cos\phi'\,d\phi'\,\hat{y}. \tag{7.36}$$

We first compute the axial component of the field. Taking the z component of the cross-product in the Biot-Savart equation, we find that the ϕ' dependence only involves terms in $\cos\phi'$. Thus symmetric current elements with respect to the x axis make identical contributions to the integral. We have

$$\begin{aligned} B_z &= \frac{\mu_0 I' a}{2\pi}\int_{-L/2}^{L/2}\int_0^{\pi}\frac{a - \rho\cos\phi'}{\{a^2+\rho^2-2a\rho\cos\phi'+(z-z')^2\}^{3/2}}\,dz'\,d\phi' \\ &= \frac{\mu_0 I' a}{2\pi}\int_0^{\pi}(a-\rho\cos\phi')\,\mathbb{I}_1\,d\phi', \end{aligned}$$

where I' is the sheet current density,

$$\mathbb{I}_1 = \int_{-L/2}^{L/2}\frac{dz'}{\{e - 2\ z\,z' + z'^2\}^{3/2}}$$

and we define

$$e = a^2 + \rho^2 - 2a\rho\cos\phi' + z^2. \tag{7.37}$$

Define the distances from the observation point to the two ends of the solenoids in terms of the new variables

$$\begin{aligned} z_1 &= -\frac{L}{2} - z \\ z_2 &= \frac{L}{2} - z. \end{aligned}$$

After doing the integration, we get[10]

$$\mathbb{I}_1 = \frac{z_2}{(e-z^2)\{a^2+\rho^2-2a\rho\cos\phi'+z_2^2\}^{1/2}} - \Omega(z_1),$$

[10] GR 2.264.5.

https://doi.org/10.1017/9781009291156.008 Published online by Cambridge University Press

where we use the symbol Ω here as a shorthand notation that means a second term similar to the first, but with L replaced by $-L$, i.e., the other end of the solenoid. Then we have

$$B_z = \frac{\mu_0 I' a}{2\pi} \int_0^{\pi} \frac{a - \rho \cos\phi'}{(a^2 + \rho^2 - 2a\rho\cos\phi')} \frac{z_2}{\left\{a^2 + \rho^2 + z_2^2 - 2a\rho\cos\phi'\right\}^{1/2}} d\phi' - \Omega(z_1).$$

Change the integration variable using

$$\begin{aligned} \cos\phi' &= -1 + 2x^2 \\ d\phi' &= -\frac{2}{\sqrt{1-x^2}}\, dx. \end{aligned} \tag{7.38}$$

This gives

$$B_z = \frac{\mu_0 I' a}{\pi} \int_0^1 \frac{a + \rho - 2\rho x^2}{[(a+\rho)^2 - 4a\rho x^2]} \frac{z_2}{\left\{(a+\rho)^2 + z_2^2 - 4a\rho x^2\right\}^{1/2}\sqrt{1-x^2}} dx - \Omega(z_1).$$

We can put the integral into a standard form by defining

$$k^2 = \frac{4a\rho}{(a+\rho)^2 + z_2^2} \tag{7.39}$$

and

$$n = \frac{4a\rho}{(a+\rho)^2}. \tag{7.40}$$

We find that

$$B_z = \frac{\mu_0 I' a}{\pi(a+\rho)^2} \frac{z_2}{\left\{(a+\rho)^2 + z_2^2\right\}^{1/2}} [(a+\rho)\ \mathbb{I}_2 - 2\rho\, \mathbb{I}_3] - \Omega(z_1),$$

where[11]

$$\begin{aligned} \mathbb{I}_2 &= \int_0^1 \frac{dx}{(1 - n x^2)\{(1 - k^2x^2)\ (1 - x^2)\}^{1/2}} \\ &= \Pi(k, -n). \end{aligned}$$

The function $\Pi(k, n)$ is the complete elliptic integral of the third kind. The other integral is

[11] GR 8.111.4.

https://doi.org/10.1017/9781009291156.008 Published online by Cambridge University Press

$$\mathbb{I}_3 = \int_0^1 \frac{x^2}{(1 - n\,x^2)\{(1 - k^2x^2)\,(1 - x^2)\}^{1/2}}\,dx.$$

This can be evaluated by writing it in the form

$$\begin{aligned}\mathbb{I}_3 &= \frac{1}{n}\int_0^1 \frac{1 - nx^2 - 1}{(1 - n\,x^2)\{(1 - k^2x^2)\,(1 - x^2)\}^{1/2}}\,dx \\ &= \frac{1}{n}\,K(k) - \frac{1}{n}\,\Pi(k, n),\end{aligned}$$

where[12]

$$K(k) = \int_0^1 \frac{dx}{\{(1 - k^2x^2)\,(1 - x^2)\}^{1/2}}\,. \tag{7.41}$$

Substituting, we find that the axial field of the solenoid is [22]

$$B_z = \frac{\mu_0 I'}{\pi}\,\frac{a\,z_2}{(a+\rho)\{(a+\rho)^2 + z_2^2\}^{1/2}}\left[K(k) + \frac{a-\rho}{2a}\left(\Pi(k, -n) - K(k)\right)\right] - \Omega(z_1). \tag{7.42}$$

Selecting instead the x component of the cross-product in the Biot-Savart equation, the transverse component of the solenoid field is

$$\begin{aligned}B_\rho &= \frac{\mu_0 I' a}{2\pi}\int_{-L/2}^{L/2}\int_0^\pi \frac{(z - z')\cos\phi'}{\{a^2 + \rho^2 - 2a\rho\cos\phi' + (z - z')^2\}^{3/2}}\,dz'\,d\phi' \\ &= \frac{\mu_0 I' a}{2\pi}\int_0^\pi \cos\phi'[z\,\mathbb{I}_1 - \mathbb{I}_4]\;\,d\phi'.\end{aligned}$$

The integral over z' involves the integral $\mathbb{I}_1$ that we have already considered and the integral[13]

$$\begin{aligned}\mathbb{I}_4 &= \int_{-L/2}^{L/2} \frac{z'}{\{e - 2\;z\,z' + z'^2\}^{3/2}}\,dz' \\ &= \frac{e - \dfrac{z\,L}{2}}{(e - z^2)\left\{a^2 + \rho^2 - 2\;a\rho\cos\phi' + \left(\dfrac{L}{2} - z\right)^2\right\}^{1/2}} - \Omega(-L),\end{aligned}$$

[12] GR 8.111.2 and 8.112.1. [13] GR 2.264.6.

https://doi.org/10.1017/9781009291156.008 Published online by Cambridge University Press

where e was defined in Equation 7.37. Substituting these back into the equation for B_ρ and simplifying, we get

$$B_\rho = \frac{\mu_0 I' a}{2\pi} \int_0^\pi \frac{\cos\phi'}{\{a^2 + \rho^2 + z_2^2 - 2a\rho\,\cos\phi'\}^{1/2}}\, d\phi' - \Omega(z_1).$$

Making the change of variable in Equation 7.38, we find

$$\begin{aligned} B_\rho &= \frac{\mu_0 I' a}{\pi}\ \frac{1}{\{(a+\rho)^2 + z_2^2\}^{1/2}} \int_0^1 \frac{2x^2 - 1}{\{(1 - k^2x^2)\,(1 - x^2)\}^{1/2}}\, dx - \Omega(z_1) \\ &= \frac{\mu_0 I' a}{\pi}\ \frac{1}{\{(a+\rho)^2 + z_2^2\}^{1/2}}\ [2\,\mathbb{I}_5 - K(k)] - \Omega(z_1), \end{aligned}$$

where k^2 was defined in Equation 7.39. The remaining integral is[14]

$$\begin{aligned} \mathbb{I}_5 &= \int_0^1 \frac{x^2}{\{(1 - k^2x^2)\,(1 - x^2)\}^{1/2}}\, dx \\ &= \frac{K(k) - E(k)}{k^2}. \end{aligned}$$

Substituting and simplifying, we find the transverse component of the solenoid field is [22]

$$B_\rho = \frac{\mu_0 I'}{4\pi}\ \frac{\{(a+\rho)^2 + z_2^2\}^{1/2}}{\rho} [2(K(k) - E(k)) - k^2 K(k)] - \Omega(z_1). \tag{7.43}$$

Equations 7.42 and 7.43 are exact solutions for the sheet solenoid that are valid for all points in space, except for observation points at the same radius as the current sheet. For an arbitrary field point with the cylindrical coordinates (ρ, ϕ, z), we can write the Cartesian values of the transverse field as

$$\begin{aligned} B_x &= B_\rho \cos\phi = B_\rho\, \frac{x}{\rho} \\ B_y &= B_\rho \sin\phi = B_\rho\, \frac{y}{\rho}. \end{aligned} \tag{7.44}$$

An alternate solution for the field components has also been given in terms of related functions known as generalized complete elliptic integrals.[23]

The vector potential for the sheet solenoid may also be expressed exactly in terms of elliptic integrals [22, 24] as

[14] GR 3.153.5.

https://doi.org/10.1017/9781009291156.008 Published online by Cambridge University Press

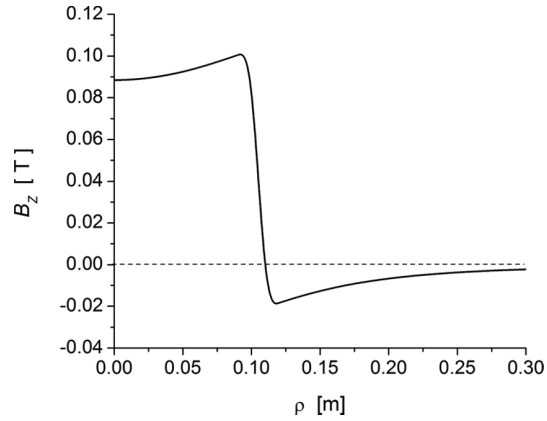

Figure 7.10 The dependence of B_z on ρ at the center of a solenoid with $L = 20$ cm, $a = 10$ cm, $I' = 10^5$ A/m.

$$A_\phi = \frac{\mu_0 I'}{4\pi}\,\frac{z_2}{\rho}\left[\{(a+\rho)^2+z_2^2\}^{1/2}(K(k)-E(k)) - \frac{(a-\rho)^2}{\{(a+\rho)^2+z_2^2\}^{1/2}}\,(\Pi(k,n)-K(k))\right] - \Omega(z_1), \tag{7.45}$$

where k and n are given by Equations 7.39 and 7.40, respectively. The vector potential and field for the sheet solenoid may also be expressed as sums of Bessel-Laplace integrals [25, 26] or in terms of modified Bessel functions.[27]

Example 7.2: radial dependence of the axial solenoid field
Let us examine the dependence of B_z on ρ at the center of a sample solenoid. The results from using Equation 7.42 are shown in Figure 7.10. Note the reversal of the field direction at the radius of the sheet.

Example 7.3: mutual inductance and axial force between a solenoid and a loop
Once the vector potential and the field components for the circular current loop and the sheet solenoid are known, the mutual inductance between a solenoid and a current loop can be computed as

$$M(S,L) = \frac{\Phi_L}{I_S} = \frac{1}{I_S}\int A_\phi(S)\,dl = \frac{2\pi\rho_L}{I_S}\,A_\phi(S),$$

where the symbols S and L refer to the solenoid and the loop.

https://doi.org/10.1017/9781009291156.008 Published online by Cambridge University Press

Assume the current is flowing in the same direction in the loop and in the solenoid. The axial force acting on a current loop due to the magnetic field from the solenoid is

$$F_z(S,L) = I_L \int \overrightarrow{dl_L} \times \vec{B}\,(S) = -I_L \int_0^{2\pi} \rho_L B_\rho(S)\; d\phi$$
$$= -2\pi I_L \rho_L B_\rho(S),$$

where the minus sign indicates that the force tries to pull the loop and the solenoid together.

7.6 Block model for the solenoid

In cases where the accuracy of the field calculated from the sheet model for the solenoid is inadequate, it may be necessary to take into account the radial thickness of the coils. Consider the cross-section of a block solenoid shown in Figure 7.11, where the coil extends from an inner radius a to an outer radius b. We can find the on-axis axial field by integrating Equation 7.31 for the field due to a current sheet

$$B_z(0,z) = \frac{\mu_0 J}{2} \int_a^b \frac{z + L/2}{\{r^2 + (z+L/2)^2\}^{1/2}}\, dr - \Omega(-L),$$

where again Ω is used as a shorthand for the expression in the first term with L replaced by $-L$. Performing the integral,[15] we find for points along the symmetry axis

$$B_z(0,z) = \frac{\mu_0 J}{2} \left\{ (z+L/2)\; \ln \left[\frac{b + \{b^2 + (z+L/2)^2\}^{1/2}}{a + \{a^2 + (z+L/2)^2\}^{1/2}} \right] \right\} - \Omega(-L). \quad (7.46)$$

The axial field at the center of the solenoid is

$$B_z(0,0) = \frac{\mu_0 J\, L}{2}\; \ln \left[\frac{b + \{b^2 + L^2/4\}^{1/2}}{a + \{a^2 + L^2/4\}^{1/2}} \right]. \quad (7.47)$$

The off-axis field from the block solenoid is usually treated by summing over the fields from a set of current sheets, using one of the methods we have previously discussed. For example, the block conductor may be simulated using a radial distribution of current sheets expressed in elliptic integrals.[22] It is also possible to express the thick solenoid field in terms of a radial expansion of the on-axis field, [9] as a series of zonal harmonics,[10, 11, 21] or in terms of Bessel-Laplace integrals.

[15] GR 2.271.5.

https://doi.org/10.1017/9781009291156.008 Published online by Cambridge University Press

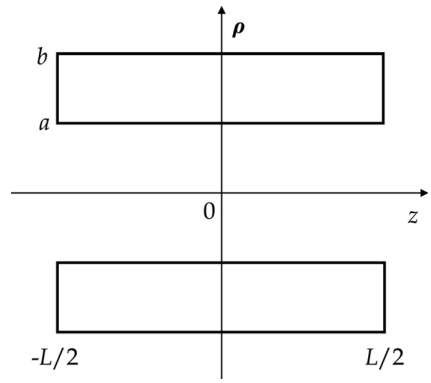

Figure 7.11 Block model of a solenoid.

[25, 26, 28] The good field region calculated for a solenoid from a properly designed block conductor is frequently larger than that for a sheet solenoid.[21]

The flux leaving a solenoid travels outside and returns through the opposite end. As a result, the fringe field on the outside of the solenoid can be quite significant. If the fringe field is unacceptable, it can be reduced by adding supplemental bucking coils or by using iron shielding. Figure 7.12 shows a POISSON model for the magnetic field in a typical solenoid. The figure shows 1/4 of a plane projection through the solenoid. The vertical axis is the centerline of the solenoid. The field is symmetric on both sides of the vertical axis and both sides of the horizontal axis. The program used Dirichlet boundary conditions on the left, right, and top borders, and Neumann boundary conditions on the bottom border. The figure on the left shows the field from just the coil, while the figure on the right illustrates the reduction in the exterior field from adding a cylindrical iron return yoke. The current in the coil was the same for both figures.

7.7 Bent solenoid

So far we have been considering configurations where current loops or solenoids have been symmetrically configured along a straight axis. In the cylindrical coordinate system we have been using, the current has been azimuthally symmetric along ϕ, the system axis has been along z, and the magnetic field only has components along ρ and z. We now generalize this to consider configurations where a solenoid, for example, is bent to follow a circular axis. The magnetic field of a bent solenoid channel is conveniently defined in terms of a rotating coordinate system that follows some reference curve, as shown in Figure 7.13. In the curvilinear description of orthogonal coordinate systems,[29] changes in the values of the coordinates (u_1, u_2, u_3) are related to the distance element by

https://doi.org/10.1017/9781009291156.008 Published online by Cambridge University Press

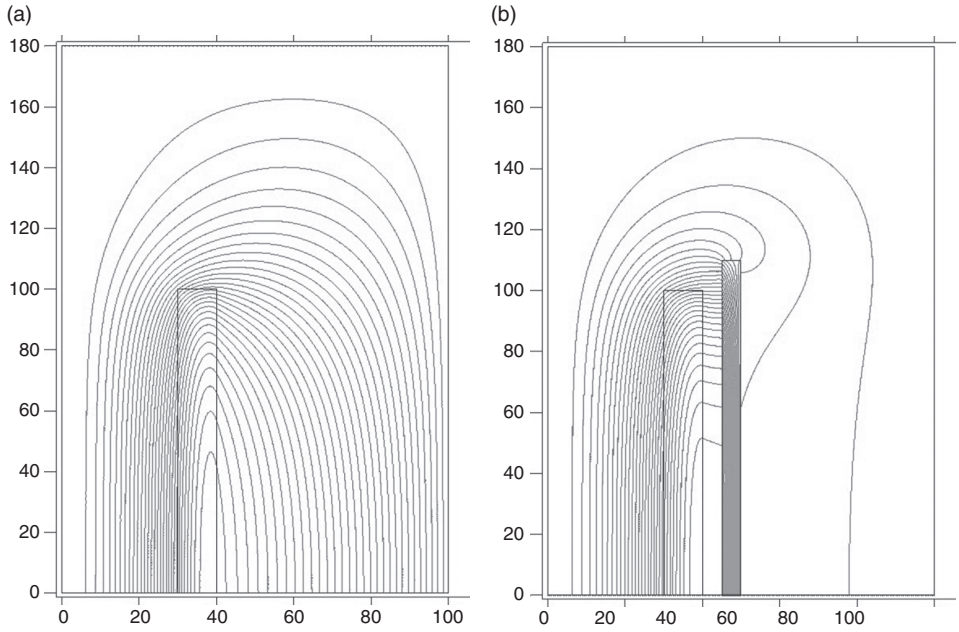

Figure 7.12 Magnetic field of a solenoid coil (left); field for a coil surrounded by an iron return path (right).

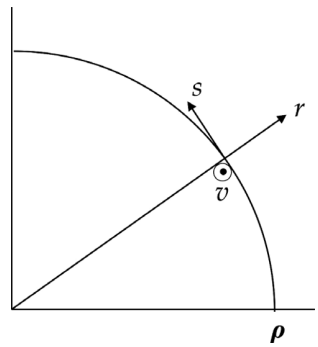

Figure 7.13 Frenet-Serret coordinate system.

$$ds^2 = h_1^2\, u_1^2 + h_2^2\, u_2^2 + h_3^2\, u_3^2,$$

where (h_1, h_2, h_3) are a set of scale factors. In the Frenet-Serret coordinate system considered here,[30, 31] the reference curve is a circle and the origin of the unit vectors moves along the circle. The unit vector s is in the bending plane and tangent to the circle. The unit vector r is in the bending plane and perpendicular to s. The unit vector v is perpendicular to the bending plane. The curvilinear scale factors are

https://doi.org/10.1017/9781009291156.008 Published online by Cambridge University Press

$$h_r = h_v = 1$$
$$h_s = 1 + \frac{r}{\rho},$$

where ρ is the radius of curvature.

We can approximate the scalar potential in the magnet aperture in terms of a power series. To compute the first-order fields, we must include second-order terms in the potential,

$$V = \mu_0 V_m \simeq V_{00} + V_{10} r + V_{01} v + V_{20} r^2 + V_{11} rv + V_{02} v^2 \ .$$

We also include terms in the potential that allow for the possibility of superimposed transverse fields. The gradient of V is defined as

$$\nabla V = \partial_r V \, \hat{r} + \frac{1}{h_s} \, \partial_s V \, \hat{s} + \partial_v V \, \hat{v}.$$

Thus the magnetic field components are

$$\begin{aligned} -B_r &\simeq V_{10} + 2V_{20} r + V_{11} v \\ -B_v &\simeq V_{01} + V_{11} r + 2V_{02} v \\ -B_s &\simeq \frac{1}{h_s} (V'_{00} + V'_{10} r + V'_{01} v + V'_{20} r^2 + V'_{11} rv + V'_{02} v^2), \end{aligned}$$

where primes indicate derivatives with respect to s. Recalling the midplane expansions of the transverse field components given in Equation 4.9, we can associate the potential terms with the multipole field coefficients[16]

$$\begin{aligned} V_{01} &= -B_1 \\ V_{10} &= A_1 \\ V_{11} &= -B_2 \\ 2V_{20} &= A_2. \end{aligned}$$

Thus to the first-order, the field components are

$$\begin{aligned} B_r &\simeq -A_1 - A_2 \, r + B_2 \, v \\ B_v &\simeq B_1 + B_2 \, r - 2 \ V_{02} \, v \\ B_s &\simeq \frac{1}{h_s} \, (b_s - A'_1 \, r + B'_1 \, v), \end{aligned} \tag{7.48}$$

[16] In the case where a charged particle has to follow the reference path in the horizontal plane, we must have the horizontal dipole field $A_1(s) = 0$.

https://doi.org/10.1017/9781009291156.008 Published online by Cambridge University Press

where we identify the on-axis component of the axial field as

$$b_s = -V'_{00}$$

and assume the transverse dipole fields can vary with s.

At this point, we still have one unidentified potential term V_{02} in Equation 7.48, so we demand that the field components also satisfy the divergence relation $\nabla \cdot \overrightarrow{B} = 0$. In the coordinates discussed here, this can be written as

$$\frac{1}{h_s}\,\partial_r(h_s B_r) + \frac{1}{h_s}\,\partial_s B_s + \partial_v B_v = 0.$$

Inserting the field components from Equation 7.48 and using

$$\frac{1}{h_s} \simeq 1 - \frac{r}{\rho},$$

we find the constraint

$$-A_2 - \frac{1}{\rho}\,A_1 - 2\;V_{02} + b'_s = 0.$$

Thus the first-order vertical field component is

$$B_v \simeq B_1 + B_2\, r - \left(b'_s - \frac{A_1}{\rho} - A_2\right) v. \tag{7.49}$$

If no superimposed transverse fields are present, the first-order axial field in the bent channel is

$$B_s \simeq b_s - \frac{r}{\rho}\, b_s. \tag{7.50}$$

It is also possible to define an expansion for the field that makes use of "curved multipoles" that directly correspond to the solution of Laplace's equation in the curved coordinate system.[32]

7.8 Toroid

When the bent solenoid channel is extended to form a closed circular ring, we have a *toroid*, as shown in Figure 7.14. The current loops from the solenoid are centered on the circular system axis and the plane of the loops lie in the ρ-z plane. The direction of the unit vectors $\hat{\rho}$ and $\hat{\phi}$ depend on the azimuthal location around the toroid. Since the coils are closer together on the side nearer to the center of

https://doi.org/10.1017/9781009291156.008 Published online by Cambridge University Press

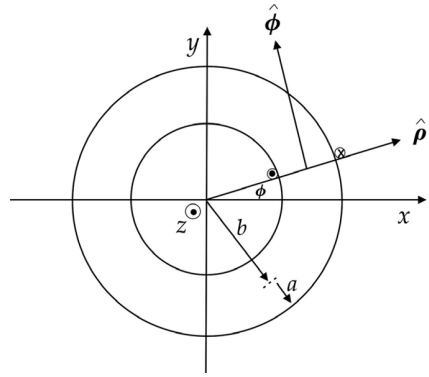

Figure 7.14 Geometry of the toroid from above.

curvature, we expect that the field inside the bent solenoid will have a gradient with respect to the system axis, in agreement with Equation 7.50.

Because of the symmetry of the configuration, all of the field components must be independent of the azimuthal angle ϕ. Let the mean radius of the toroid equal b and the radius of the current loops equal a. Then a simple application of the Ampère law on the midplane ($z = 0$) shows that $B_\phi = 0$ for $\rho < b - a$ and for $\rho > b + a$ since no net current is enclosed in a circular path in those regions. However, applying the Ampère law on a circular path on the midplane, we find the field inside the toroid is

$$B_\phi = \frac{\mu_0 N I}{2\pi\rho}, \tag{7.51}$$

where N is the number of conductor turns around the circumference and ρ is the radius of the path. This shows that the field varies like $1/\rho$ inside the toroid.

A cross-section of the toroid at some azimuthal angle ϕ is shown in Figure 7.15a. The angle α gives the location of an element of the current loop. The current element has the Cartesian coordinates

$$\begin{aligned} x_l &= (b + a\,\cos\alpha)\,\cos\phi \\ y_l &= (b + a\,\cos\alpha)\,\sin\phi \\ z_l &= a\sin\alpha \end{aligned}$$

and the directions

$$\begin{aligned} dl_x &= a\,\sin\alpha\,\cos\phi\,d\alpha \\ dl_y &= a\,\sin\alpha\,\sin\phi\,d\alpha \\ dl_z &= -a\,\cos\alpha\,d\alpha. \end{aligned}$$

https://doi.org/10.1017/9781009291156.008 Published online by Cambridge University Press

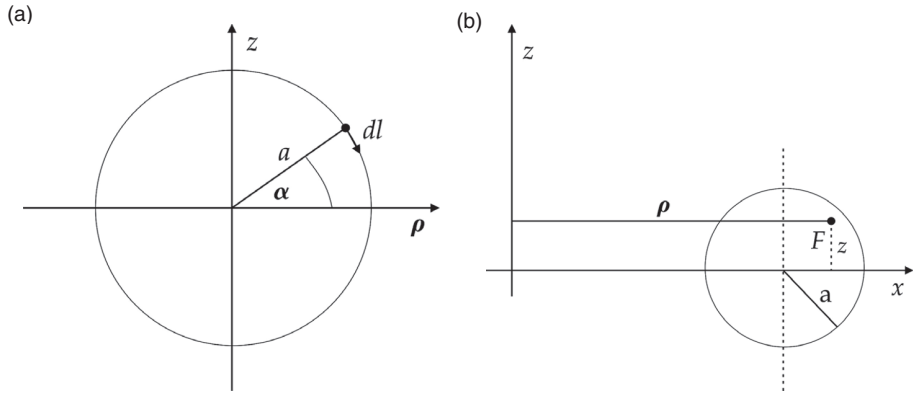

Figure 7.15 (a) Cross-section of the toroid at the azimuthal location ϕ; (b) location of the field observation point *F*.

The location of the field observation point (ρ, 0, z) is shown in Figure 7.15b. The resulting distance vector is

$$\overrightarrow{R} = [\rho - (b + a\cos\alpha)\cos\phi]\,\hat{x} - (b + a\cos\alpha)\sin\phi\,\hat{y} + (z - a\sin\alpha)\,\hat{z}.$$

Applying the Biot-Savart law to any point inside the toroid shows that B_z and B_ρ vanish. It follows that the field inside the toroid has to have the form

$$B = B_\phi(\rho, z).$$

The analytic results for B_ϕ are complicated [33] expressions defined in terms of integrals of elliptic integrals. Alternatively, one could examine the field inside the toroid by evaluating one of the integrals in terms of complete elliptic integrals and performing the other integral numerically.

References

[1] W. Smythe, *Static and Dynamic Electricity*, 2nd ed., McGraw-Hill, 1950, p. 270–275.
[2] J. Stratton, *Electromagnetic Theory*, McGraw-Hill, 1941, p. 263.
[3] R. Good, Elliptic integrals, the forgotten functions, *Eur. J. Phys.* 22:119, 2001.
[4] W. Panofsky & M. Phillips, *Classical Electricity and Magnetism*, 2nd ed., Addison-Wesley, 1962, p. 156.
[5] R. Schill, General relation for the vector magnetic field of a circular current loop: a closer look, *IEEE Trans. Magnetics* 39:961, 2003.
[6] J. D. Jackson, *Classical Electrodynamics*, Wiley, 1962, p. 142.
[7] D. Redzic, The magnetic field of a static current loop: a new derivation, *Eur. J. Phys.* 27:N9, 2006.
[8] G. Harnwell, *Principles of Electricity and Magnetism*, 2nd ed., McGraw-Hill, 1949, p. 329.

https://doi.org/10.1017/9781009291156.008 Published online by Cambridge University Press

[9] R. Jackson, Off-axis expansion solution of Laplace's equation: application to accurate and rapid calculation of coil magnetic fields, *IEEE Trans. Electron Devices* 46:1050, 1999.
[10] M. Garrett, Axially symmetric systems for generating and measuring magnetic fields, *J. Appl. Phys.* 22:1091, 1951.
[11] F. Gluck, Axisymmetric magnetic field calculation with zonal harmonic expansion, *Progress in Electromagnetics Research B* 32:351, 2011.
[12] G. Arfken, *Mathematical Methods for Physicists*, 3rd ed., Academic Press, 1985, equation 12.25.
[13] Ibid., equation 12.24.
[14] L. Eyges, *The Classical Electromagnetic Field*, Dover, 1980, p. 140.
[15] J. Wang, S. She & S. Zhang, An improved Helmholtz coil and analysis of its magnetic field homogeneity, *Rev. Sci. Inst.* 73:2175, 2002.
[16] J. Higbie, Off-axis Helmholtz field, *Am. J. Phys.* 46:1075, 1978.
[17] E. Purcell, Helmholtz coils revisited, *Am. J. Phys.* 57:18, 1989.
[18] P. Murgatroyd, Optimum designs of circular coil systems for generating non-uniform axial magnetic fields, *Rev. Sci. Inst.* 50:668, 1979.
[19] P. Murgatroyd & B. Bernard, Inverse Helmholtz pairs, *Rev. Sci. Inst.* 54:1736, 1983.
[20] R. Merritt, C. Purcell & G. Stroink, Uniform magnetic field produced by three, four and five square coils, *Rev. Sci. Inst.* 54:879, 1983.
[21] M. Garrett, Thick cylindrical coil systems for strong magnetic fields with field or gradient homogeneities of the 6th to 20th order, *J. Appl. Phys*. 38:2563, 1967.
[22] M. Garrett, Calculation of fields, forces and mutual inductances of current systems by elliptic integrals, *J. Appl. Phys.* 34:2567, 1963.
[23] N. Derby & S. Olbert, Cylindrical magnets and ideal solenoids, *Am. J. Phys.* 78:229, 2010.
[24] L. Cohen, An exact formula for the mutual inductance of coaxial solenoids, *Bulletin Bureau Standards* 3:295, 1907.
[25] J. Conway, Exact solutions for the magnetic fields of axisymmetric solenoids and current distributions, *IEEE Trans. Mag.* 37:2977, 2001.
[26] J. Conway, Trigonometric integrals for the magnetic field of a coil of rectangular cross section, *IEEE Trans. Mag.* 42:1538, 2006.
[27] T. Tominaka, Magnetic field calculation of an infinitely long solenoid, *Eur. J. Phys.* 27:1399, 2006.
[28] V. Labinac, N. Erceg & D. Kotnik-Karuza, Magnetic field of a cylindrical coil, *Am. J. Phys.* 74:621, 2006.
[29] W. Panofsky & M. Phillips, *op. cit*., p. 473–476.
[30] S. Y. Lee, *Accelerator Physics*, World Scientific, 1999, p. 33–34.
[31] C. Wang & L. Teng, Magnetic field expansion for particle tracking in a bent solenoid channel, Proc. 2001 *Particle Accelerator Conference*, p. 456. Available from www .jacow.org.
[32] S. Mane, Solutions of Laplace's equation in two dimensions with a curved longitudinal axis, *Nuc. Instr. Meth. A* 321:365, 1992.
[33] N. Carron, On the fields of a torus and the role of the vector potential, *Am. J. Phys.* 63:717, 1995.